Residual Stress Depth Profiling of Commercially Pure Titanium Subjected to High-Speed Machining Using Energy Dispersive Diffraction

N. Janse van Rensburg, D.M. Madyira, R.F. Laubscher, G.A. Oosthuizen,
Department of Mechanical Engineering Science, University of Johannesburg, South Africa

Abstract
Residual stress is well-known to influence the mechanical properties of machined components. The magnitude and distribution of these stresses are critical to determine the component's life, specifically under fatigue loading. There exists a growing need to better understand the effects of cutting parameters on residual stress and to identify more innovative methods to evaluate residual stress. Titanium has been widely used, but many of the same qualities that enhance titanium's appeal for most applications also contribute to it being one of the most difficult to machine materials. High-speed cutting experiments were conducted on commercially pure (CP) titanium and the residual stress depth profile was analysed using energy dispersive diffraction (EDDI). The residual stress depth profile of CP Grade 4 titanium was then evaluated. Experimental results show that cutting speed and depth of cut have a significant effect on the residual stress profile. At a low cutting speed, the surface residual stresses are largely compressive, becoming less compressive with an increase in cutting speed. An increase in depth of cut also introduces more compressive residual stresses into the material.

Keywords
Residual Stress, Commercially Pure Titanium, Grade 4, Energy Dispersive Diffraction

1 INTRODUCTION

Titanium and its alloys are extensively used in the aerospace, biomedical and automotive industries [1, 2, 3]. These widespread applications are due to their excellent mechanical properties and biocompatibility [4, 5]. Commercially Pure (CP) titanium found a niche in medical applications [3, 4]. This is mainly due to its superior biocompatibility, osseo-integration properties, high chemical inertness of the oxide that covers its surfaces and its mechanical properties compared to other metallic implant materials [3, 6, 7]. The demand for long lasting implants has increased significantly in the past decade and it is projected that the demand for some implants could grow by as much as 600% from the present rate by 2030 [8]. The machinability of Titanium (Ti) alloys still remains a challenge, because of the material's high temperature chemical reactivity, low thermal conductivity and low modulus of elasticity [9]. The material's low thermal conductivity results in rapid heat build-up and strong adhesion at the tool/work interface. The high chemical reactivity causes the Ti-material to weld onto the cutting tool; or for diffusion to occur between the materials. Work hardening also occurs, causing titanium to exhibit little or no edge built-up, resulting in a high shear angle and a small chip-tool contact area [5, 10]. Material characteristics and the complexity of the design of titanium components also add to the cost of machining, since a considerable amount of stock material has to be removed from primary forms such as forgings, plates and bars. In some instances, as much as 90% plus of the primary form's weight are removed. The material is therefore generally considered as difficult to machine (see Figure 1 [11]).

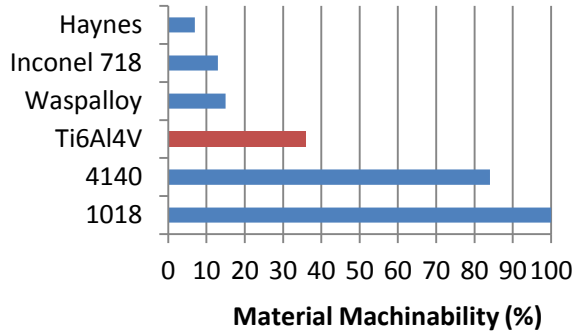

Figure 1 - Comparison of the machinability ratings of some popular materials [11]

The high cost associated with the use of titanium and its alloys is attributed to the complexity of the extraction process, as well as difficulties experienced during melting, fabrication and processing. Machining is an important value-adding process in the manufacturing of titanium components. Low cutting speeds, low feed rates and excessive tool wear also add to the cost associated with the machining of titanium and its alloys [12]. Therefore, machining of Ti-materials is generally time consuming and consumable intensive [13]. Manufacturing processes to change the shape or modify the component's surface and microstructure, subsequently result in temperature

gradients and/or plastic deformation. These alterations induce residual stress fields on the surface and in sub-surface layers of the shaped part. The increased problem of strong adhesion at the tool/work interface, at elevated temperatures and low thermal conductivity of titanium contribute to the emergence of non-uniform, high residual stresses on the surface and subsurface of Ti-components [14]. Since Ti-alloys are used in the aerospace industry the characteristics of the machined surface have to conform to aerospace regulations [15] for these applications. If the work piece is exposed to oxygen and nitrogen at high temperature (high v_c), these elements will diffuse into the base material and make the components brittle. Both oxygen and nitrogen stabilize the α-phase and create a so called α-case, on the surface of the work piece. This forms part of the effect known as material burn and a test called 'Blue Etch Method' has been developed [16] to detect the brittle parts. Surface integrity involves the outermost surface layers of a machined component (see Figure 2). It consists of topography effects such as surface roughness (R_a), changes in the metallurgy (phase transformations and inclusions) and the introduction of other surface layers such as oxides and contaminants. Mechanical effects such as voids and cracks; and deformation layers that influence the mechanical property changes (typically hardness) also play a role.

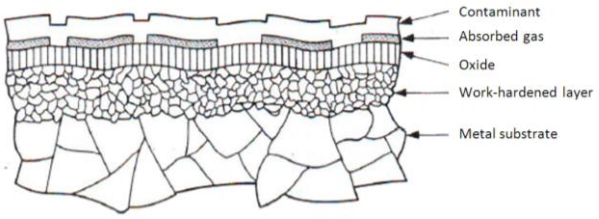

Figure 2 - Typical cross section of a machined surface [17]

The depth and the properties of the work-hardened layer that lies above the substrate are a result of the machining conditions. Residual stresses occur in the vicinity of this layer of the surface, if the material is subjected to non-uniform deformation or severe temperature gradients [18]. A thin oxide film, which is always created on a Ti-surface, forms above the work-hardened layer [19]. These oxide layers are generally much harder than the substrate making oxides brittle and abrasive [18]. If the α-case exists, it is formed beneath this thin oxide film. The presence of these stress fields can have a significant effect on the performance of the component. Generally, a process that results in near surface residual compression is beneficial and enhances resistance to failure. In contrast, a process that produces residual surface tension usually aids the onset of cracking which in turn can adversely influence the fatigue life of a component [20]. Knowledge of the residual stress state in a machined component can be critical for quality control of surface engineering processes and is considered essential when performing an accurate assessment of component life under fatigue loading. Furthermore, residual stresses locked-in after material processing can also affect the corrosion characteristics of a component. In order to predict the influence of residual stress fields on a material or component's behaviour, it is essential to have an accurate knowledge of the depth, magnitude and direction of the stresses generated. Practically all fatigue failure initiates at the surface and there is ample evidence that fatigue properties are sensitive to surface conditions. Factors which affect the surface fatigue of a component can be roughly divided into three categories, (1) surface roughness, (2) alteration of the fatigue strength of the surface metal, and (3) the residual stress condition of the surface [21, 4, 11]. Oxidation and corrosion also add to the deterioration of the fatigue properties. In order to stay competitive in the Ti-machining market, manufacturing companies generally tend to focus on high precision and effective small volume production of complex Ti-components. It is considered essential to achieve the highest machining efficiency, while minimizing the costs associated when machining Ti-components. In order to add even more value and further expand the production of Ti-components, deeper insight into the residual stress distribution of machined components are required to ultimately surface engineer these components to the preferred compressive residual stress profile. Therefore, it is important to evaluate the effect of varying cutting parameters on the residual stress profile of these components, to insure high quality finished parts. The challenge is that there remains an unspecified intermediate region with respect to the accessible near surface zone, ranging between 10-100 μm, where the conventional X-ray methods are no longer effective and the neutron methods are not yet sensitive [22]. In this research study the effect of high cutting speeds on the surface finish and residual stress depth profile of CP titanium (Grade 4 - UNS R50700) were investigated using energy dispersive diffraction (EDDI) techniques. Applying EDDI in reflection geometry, using white synchrotron radiation between about 10 and 100 keV, allows for residual stress evaluation in the intermediate surface zone (at approximately 10-100 μm). Based on the sin2ψ-measuring technique, the residual stress depth profiles of machined CP titanium were evaluated. The surface roughness was also measured and R_a data recorded.

2 COMMERCIALLY PURE TITANIUM

Titanium exists in two allotropic modifications: a high-temperature, body-centered crystalline (BCC) lattice and a low-temperature hexagonal close-packed (HCP) lattice. Titanium alloys are also divided into four categories by phase composition, namely α-alloys, near α-alloys, α/ß-alloys and ß-alloys [23]. A-Titanium exists at temperatures below

882°C, and β-titanium at higher temperatures up to the melting point [21]. This investigation will focus on CP grade titanium with a HCP α-phase structure. Single-phase α-alloys are solid solution strengthened by the addition of α-stabilizers or neutral alloying elements. The α-alloys are stable and have desired high temperature properties, but are not amenable to heat treatment for microstructural property modifications. As a single-phase material, CP grade titanium's properties are controlled by chemistry (iron and interstitial impurity elements) and grain size. CP titanium is classified into grades 1 to 4, depending on the strength and allowable levels of the elements iron, carbon, nitrogen, and oxygen. Of these grades CP (Grade 4) titanium is the strongest, with a minimum yield strength of 485 MPa [10]. It also has the highest allowable oxygen and iron content of the Ti-grades. CP (Grade 4) combines the excellent resistance to corrosion and corrosion fatigue with high strength. It is not subject to grain boundary embrittlement or sensitization at elevated temperatures, which makes it competitive with stainless steels and nickel alloys in many corrosion resistant applications [4]. Considering the specific strength of the material, CP titanium (Grade 4) outperforms S3169 austenitic stainless [11, 5]. Thermal properties for CP titanium are presented in Table 1. These unique properties also result in high cutting temperature, short tool life and high levels of tool vibration, similar to most Ti-alloys.

Thermal conductivity [$W.m^{-1}.K^{-1}$]	Thermal Expansion Co-efficient		Beta Transus [°C±15]	Melt Range [°C±15]
	0-100°C [10^{-6} K^{-1}]	0-300°C [10^{-6} K^{-1}]		
16.3	8.6	9.2	949	1660

Table 1 - Thermal properties of CP titanium

Difficulties experienced during machining include high cutting temperatures and high cutting forces in the immediate vicinity of the cutting edge, leading to catastrophic tool failure. Also, during machining of titanium high levels of chatter (self-induced vibration) can be experienced, due to the low modulus of elasticity of titanium, especially for finish cutting thin-walled components [11].

Slender parts tend to deflect under tool pressures, which results in rubbing rather than cutting. Rigidity of the entire system is consequently important, as is the use of sharp, properly shaped cutting tools. In general, low cutting speeds, heavy feed rates, and copious amounts of cutting fluid are recommended when cutting titanium and its alloys [15].

3 RESIDUAL STRESS AND ENERGY-DISPERSIVE DIFFRACTION

Knowledge of the magnitude and distribution of residual stress fields in a component is considered essential when assessing fatigue life. Non-destructive, phase selective analysis of residual stresses caused by material processing in polycrystalline samples is usually performed by diffraction. Elastic strains are measured and residual stresses are calculated from the elastic properties of the materials concerned. Diffraction techniques can employ conventional X-rays, synchrotron radiation or neutrons [24]. The determination of residual stresses requires a detailed understanding of the processes responsible for the stresses and of the elastic and plastic properties of the materials being investigated. Using X-ray and neutron probes, respectively, complementary information on the residual stress distribution in the near surface region and the volume of the material is available. Residual stress evaluations of machined samples were conducted at the Berlin synchrotron storage ring, known as the BESSY. This storage ring utilizes an energy dispersive diffraction (EDDI) technique. The EDDI beamline utilizes a high energy white photon beam with a 13.5 keV critical energy at 1.7 GeV provided by a 7T multipole wiggler [22].

4 EXPERIMENTAL SETUP AND DESIGN

In order to determine the residual stress after cutting, the CP titanium samples were prepared by machining two billets (Ø=75 mm) using an Efamatic CNC turning lathe with a maximum spindle speed of 6000 r/min. The properties of the CP titanium are shown in Table 2. An initial cut (clean cut) with a depth of cut of 1mm at 70 m/min was performed before sample cutting commenced to imitate primary machining operations and to ensure a uniform cutting surface on both billets.

Density	Tensile strength	Yield strength (σ_y)	Elastic modulus
[kg/m^3]	[MPa]		[GPa]
4540	700	550	104.1

Table 2 - Properties of the experimental CP titanium (Grade 4)

The samples were machined over a 25mm span of the billet (with approx. 30m total cut length) to ensure stable machining conditions as shown in Table 3. The cutting speeds were varied from 70 to 300 m/min at a fixed feed rate of 0.2 mm/rev.

Depth of cut	*DOC*	0.25 mm & 1 mm
Feed rate	f_n	0.2 mm/rev
Cutting speed	v_c	70-300 m/min
Cut length	*l*	30 m

Table 3 - Cutting parameters for the experiments

So-called roughing cuts were conducted at a depth of cut of 1 mm, while it was reduced to 0.25mm for finishing cuts. Cemented tungsten carbide H1P (Sandvik Coromant) tool inserts, without chip breaker technology were used. A new cutting tool

surface edge was used with each cut, to ensure comparable results. These 80° rhombic shaped inserts have a tool nose radius of 0.8 mm and an entry angle of 95°. The cutting force and tool temperature were recorded to identify any mechanical or thermal irregularities during the cutting operations. Surface roughness measurements were conducted after machining using a Hommeltester T8000 R60-400. The surface roughness average (R_a) values were documented for comparison. Sections of the billet were removed by wire EDM to ensured minimal disturbance of the turning induced residual stresses. A schematic of the experimental is shown in Figure 3. A 1×1 mm^2 photon beam is generated that is reduced to 0.5×0.5 mm^2 at the experimental station. It has the capacity to resolve residual stresses for titanium up to a depth of 100 µm.

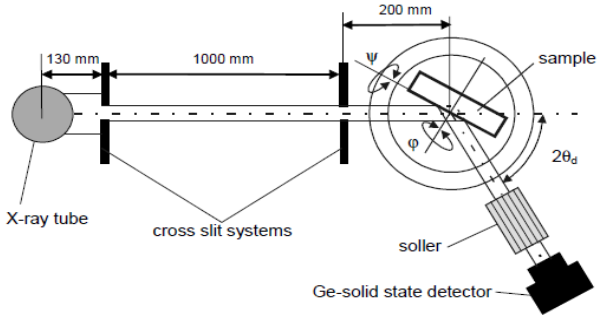

Figure 3 - Schematic view of the experimental setup at the synchrotron storage ring, known as the BESSY

The average measurement volume was 50 μm^3. The specimen was mounted on a 5-axis Eulerian saddle (shown in Figure 4) and aligned using an integrated laser pointer and CCD camera system.

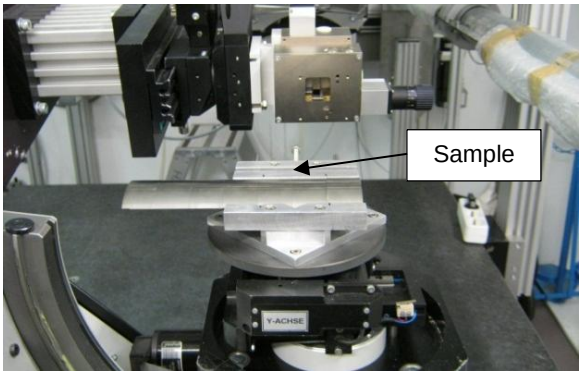

Figure 4 - CP titanium (Grade 4) sample mounted for EDDI residual stress evaluation

For each 25 mm span, three measurement points were selected representing the beginning (A), transition (C) and end (B) of the cutting process as shown in Figure 5. Measurements were done for φ angles of 0° and 90°, assuming no residual shear stresses at depths varying from approximately 10-100µm.

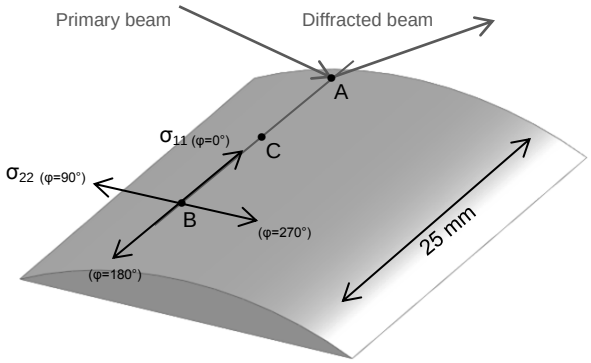

Figure 5 - Experimental sample and diffraction geometry of the EDDI test apparatus

The 0^o and 180^o orientation corresponded to the direction of the specimen which is transverse to the cutting direction (x-axis) while the 90^o and 270^o corresponded to the metal cutting direction (y-axis)0. The (psi) ψ angle was varied from 6 to 80° in order to alter the scattering vector. Data sampling for the four directions at each point took approximately one hour.

5 EXPERIMENTAL RESULTS AND DISCUSSION

Typical representative residual stress data from the EDDI for σ_{11} and σ_{22} are presented as a function of depth (τ) in Figure 5 and 6. The legends in these figures show the most dominant reflection angle at a specific depth (τ) from the surface of the material. In general the near surface residual stresses were compressive for all speeds and cutting depths tested. The maximum compressive residual stresses were measured near surface (13.6 µm) and tended to decrease with and increase in depth. This maximum compressive region extended to approximately 40 µm for the 0.25 mm depth of cut and approximately 60 µm for the 1.0 mm cut. The larger cut depth implies higher heat input therefore extending the affected zone. Cutting forces and tool temperatures were monitored during cutting operations. Irregularities (sudden increases in cutting forces and temperatures) were noted for the highest cutting speeds at extended cut lengths just before rapid tool degeneration (failure) occurred. The main cutting force remained largely constant as a function of cutting speed although a slight decrease was observed at the highest speeds. Typically the cutting force for the 1 mm cut decreased from approximately 410 N (70 m/min), to 375 N at 300 m/min. The 0.25 mm cut decreased from approximately 120 N to 100 N for the same speed range. This is largely because of the thermal softening effect associated with the increased heat rate at the higher cutting speeds.

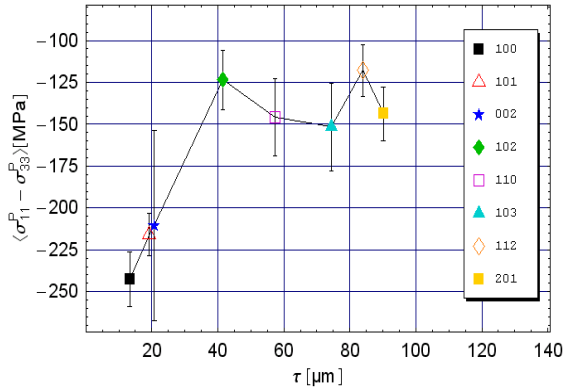

Figure 5 - EDDI Residual Stress analysis of the σ_{11} stresses of Grade 4 (300 m/min, 0.25 mm with $\sigma_{33}\approx 0$)

Surface finish was monitored but no clear trend could be observed except that the best surface finishes (Ra 1.3-1.5 µm) were obtained in the intermediate cutting speed ranges (150-250 m/min).

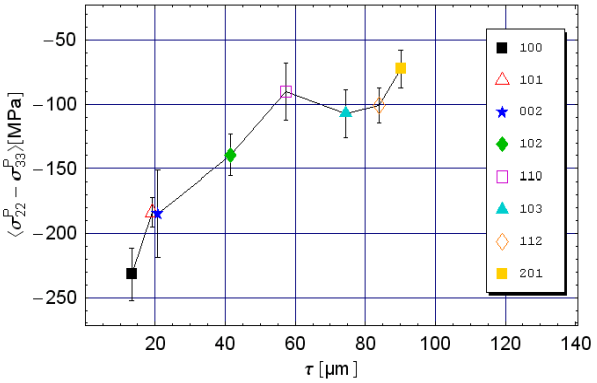

Figure 6 - EDDI Residual Stress analysis of the σ_{22} stresses of Grade 4 (300 m/min, 1 mm with $\sigma_{33}\approx 0$)

The maximum compressive residual stresses obtained (usually near surface at 13.6 µm) are plotted as a function of cutting speed in Figure 7. In general the near surface residual stress is compressive with maximum values of approximately 350 MPa measured. This corresponds to 50% of the yield stress. The residual stresses associated with the main cutting direction and the transverse direction is similar although the transverse direction is usually slightly smaller. In general an increase in cutting speed leads to a reduction of the residual stress, the highest cutting speeds displaying the lowest residual stresses. This is because of the complex interaction between the plastic deformation that tends to induce compressive residual stresses and the thermal effects that tends to induce tensile residual stress. An increase in cutting speed leads to a higher thermal load rate that leads to higher cutting temperatures. The thermal effect then starts to dominate leading to less compressive residual stresses or more tensile stresses. If it is assumed in general that compressive residual stresses are most beneficial for fatigue purposes then low to intermediate cutting speeds would lead to the most beneficial surface. This is assuming that no dramatic change in the residual stress profile occurs within the first 13.6 µm depth. The nearest actual surface stresses should therefore also be determined.

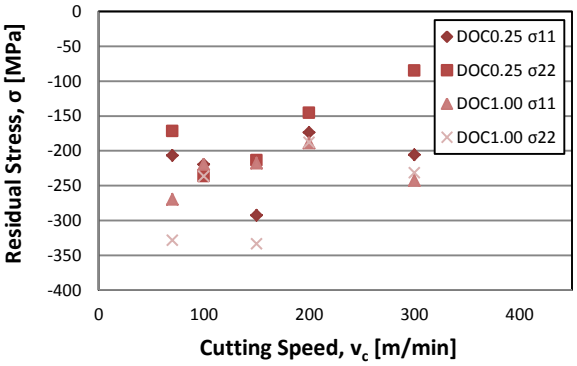

Figure 7 - Residual stress vs. cutting speed of machined CP titanium (Grade 4)

6 CONCLUSION

The EDDI technique has been shown to be an effective tool in measuring subsurface residual stress fields for Grade 4 titanium alloy between depths of 13.6 and 100 µm. Surface X-Ray diffraction and higher energy techniques should be utilized for nearest surface and extended depth probing of the machined residual stress field. In general the residual stress field for machined Grade 4 titanium alloy is compressive with maximum compressive stresses of 50% of yield measured. This field extends to approximately 50 µm's, but is a function of the cutting conditions. An increase in cutting speed leads to a reduction in the absolute compressive stress up to cutting speeds of 300 m/min.

7 ACKNOWLEDGEMENTS

The authors thank BESSY II and their staff, specifically Dr Manuela Klaus and Dr Rodrigo Coelho, for beam time and assistance with machine setup and data analysis.

8 REFERENCES

[1] D. Ulutan e T. Ozel, "Machining induced surface integrity in titanium and nickel alloys: A review," *International Journal of Machine Tools & Manufacture,* vol. 51, p. 250–280, 2011.

[2] K. Wang, "The use of titanium for medical applications in the USA," *Materials Science and Engineering,* vol. A213 , pp. 134-137, 1996.

[3] M. Geetha, A. Singh, R. Asokamani e A. Gogia, "Titanium based biomaterials, the ultimate choice for orthopaedic implants: A review," *Progress Materials Science,* vol. 54, pp. 397-425, 2009.

[4] R. Boyer, "An Overview of the Use of Titanium in the Aerospace Industry," *Materials Science & Engineering A,* vol. A213, pp. 103-114, 1996.

[5] E. Ezugwu, J. Bonney e Y. Yamane, “An Overview of the Machinability of Aeroengine Alloys,” *Journal of Materials Processing Technology,* vol. 134, pp. 233-253, 2003.

[6] F. McBagonluri e W. Soboyejo, “Titanium Alloys: Structure, Properties, and Applications,” em *Advanced Structural Materials: Properties, Design Optimization, and Applications*, Taylor & Francis Group, 2006, pp. 306-382.

[7] S. Basturk, F. Senbabaoglu, C. Islam, M. Erten, I. Lazoglu e T. Gulmez, “Titanium machining with new plasma boronized cutting tools,” *CIRP Annals - Manufacturing Technology,* vol. 59, p. 101–104, 2010.

[8] S. Kurtz, K. Ong, E. Lau, F. Mowat e H. M., “Projections of primary and revision hip and knee arthroplasty in the United States from 2005 to 2030,” *J Bone Jt Surg Am,* vol. 89, pp. 780-785, 2007.

[9] G. Oosthuizen, G. Akdogan e N. Treurnicht, “The performance of PCD tools in high-speed milling of Ti6Al4V,” *International Journal of Advanced Manufacturing Technology,* 2010.

[10] M. McCann e J. Fanning, Handbook of Mechanical Alloy Design, Henderson, Nevada: TIMET Henderson Technical Laboratory, ****.

[11] G. Oosthuizen, G. Akdogan, D. Dimitrov e N. Treurnicht, “A Review of the Machinability of Titanium alloys,” *R&D Journal of the South African Institution of Mechanical Engineering,* vol. 26, n.º 1, pp. 43-52, 2010.

[12] C. Dandekar, Y. Shin e J. Barnes, “Machinability improvement of titanium alloy (Ti–6Al–4V) via LAM and hybrid machining,” *International Journal of Machine Tools & Manufacture,* vol. 50, p. 174–182, 2010.

[13] S. Sun, M. Brandt e M. Dargusch, “Characteristics of cutting forces and chip formation in machining of titanium alloys,” *International Journal of Machine Tools & Manufacture,* vol. 49, p. 561–568, 2009.

[14] N. Valentin, Titanium Alloys: Russian Aircraft and Aerospace Applications, CRC Press, 2006.

[15] G. Oosthuizen, “Wear characterisation in milling of Ti6Al4V - A wear map approach,” Stellenbosch University, Stellenbosch, South Africa, 2010.

[16] A. McEvily, “Failures in inspection procedures: case studies,” *Engineering Failure Analysis,* vol. 11, n.º 1, p. 167–176, 2004.

[17] S. Kalpakjan, Manufacturing Engineering and Technology, Addison-Wesley Publishing, 1995.

[18] S. Van Trotsenburg e R. Laubscher, “The effect of high speed machining on the surface integrity of certain titanium alloys,” em *COMA'10 International Conference on Competitive Manufacturing*, Stellenbsoch, 2010.

[19] S. Kuriakose e M. Shunmugam, “Characteristics of Wire Electro-discharge Machined Ti6Al4V Surface,” *Materials Letters,* vol. 58, pp. 2231-2237, 2004.

[20] T. Kitagawa, A. Kubo e K. Maekawa, “Temperature and Wear of cutting tools in High-speed Machining of Inconel 718 and Ti-6Al-6V-2Sn,” *Wear,* vol. 202, n.º 2, pp. 142-148, 1997.

[21] E. Ezugwu e Z. Wang, “Titanium Alloys and their Machinability - A Review,” *Journal of Materials Processing Technology,* vol. 68, n.º 3, pp. 262-274, 1998.

[22] C. Genzel, C. Stock e W. Reimers, “Application of energy-dispersive diffraction to the analysis of multiaxial residual stress fields in the intermediate zone between surface and volume,” *Materials Science and Engineering A,* p. 28–43, 2004.

[23] C. Chunxiang, H. BaoMin e L. Shuangjin, “Titanium alloy production technology, market prospects and industry development,” *Materials and Design,* vol. 32, n.º 3, pp. 1684-1691, March 2011.

[24] M. Fitzpatrick e A. Lodini, Analysis of residual stress by diffraction using neutron and synchrotron radiation, London: Taylor & Francis, 2003.

BIOGRAPHY

Nickey Janse van Rensburg obtained a MSc in Mechanical Engineering from the North-West University in 2008 and is a lecturer in Material Science at the University of Johannesburg, South Africa.

Daniel Makundwaneyi Madyira obtained an MSc in Design of Turbomachinery from Cranfield University, United Kingdom in 1993. He is a lecturer in Strength of Materials at the University of Johannesburg, South Africa.

Rudolph Laubscher obtained his D.Ing degree in Mechanical Engineering from the Rand Afrikaans University in Johannesburg. He is currently associate professor in the Department of Mechanical Engineering Sciences at the University of Johannesburg, South Africa.

Gert Adriaan Oosthuizen obtained his PhD degree from Stellenbosch University. In 2011 he became a CIRP research affiliate and was appointed as senior lecturer at the University of Johannesburg, South Africa.